Experimental Gerontology 225 (2026) 113347

Contents lists available at ScienceDirect

Experimental Gerontology

journal homepage: www.elsevier.com/locate/expgero

# Differences of oxidative damage in the brain of short- and long-lived *Nothobranchius furzeri* strains☆

Julien Lehmann [1], Oksana Savel [1], Melissa M. Page [*]

*Louvain Institute of Biomolecular Science and Technology, UCLouvain, Louvain-la-Neuve, Belgium*

ARTICLE INFO

*Keywords:*
Mitochondrial dysfunction
Oxidative damage
Brain
*Nothobranchius furzeri*
Lifespan
Long-lived species
Short-lived species

ABSTRACT

*Background:* The turquoise killifish *(Nothobranchius furzeri)*, while being reported as the vertebrate with the shortest lifespan in captivity, includes many strains that diverge in their lifespans. Underlying mechanisms for these differences are believed to occur in part at the level of mitochondria, which contribute to aging through their role in energy metabolism and oxidative stress.

*Methods:* We used the short-lived GRZ strain and the longer-lived MZCS-222 strain to determine whether lifespan divergence is associated with distinct mitochondrial maintenance, oxidative damage, and mitigating pathways in the brain. Killifish brain homogenates were analyzed through western blots, RT-qPCR and enzymatic assays.

*Results:* In these two strains, we report that mitochondrial content declined with age in GRZ individuals, whereas it remained stable in MZCS-222 fish. The longer-lived strain also exhibited age-related increases in SOD1 and SOD2 at the protein level, suggesting enhanced antioxidant defenses. In contrast, GRZ showed an early upregulation of *pink1* and *bax*, consistent with putative increased mitophagy and apoptotic signaling in response to mitochondrial stress, whereas MZCS-222 showed an increase in *pink1* expression while maintaining stable levels of *bax*, indicating a possible control of mitochondrial quality through mitophagy only.

*Conclusion:* Together, these findings indicate that lifespan divergence in *N. furzeri* is associated with distinct mitochondrial aging trajectories, supporting that enhanced antioxidants defenses and mitochondrial quality control contribute to the preservation of brain mitochondrial homeostasis and increased longevity.

## 1. Introduction

Aging can be influenced by numerous intrinsic and extrinsic factors. Among these, environmental stress plays an important role in shaping an individual's lifespan. Indeed, resource availability, predation, and habitat stability shape life-cycle strategies and the rate of senescence (Monaghan et al., 2008). In environments where extrinsic mortality is high, organisms often exhibit rapid growth and a shortened lifespan, whereas more stable conditions can promote better cellular maintenance and greater longevity (Reznick et al., 1990). This framework is consistent with the antagonistic pleiotropy theory, in which certain genes that promote early life advantages, such as rapid growth, may have deleterious effects later in life and thereby contribute to cellular and molecular aging (Kirkwood and Austad, 2000; Williams, 1957).

In this context, *Nothobranchius furzeri*, also known as the turquoise killifish, represents a unique in vivo model to study aging. Indeed, its naturally short lifespan, together with the existence of strains with marked differences in lifespan and the development of similar aging hallmarks, provides a unique opportunity to investigate mechanisms that shape aging (Cellerino et al., 2016; Hu and Brunet, 2018; Polačik et al., 2014; Savel et al., 2026). Wild populations of *N. furzeri* inhabit temporary ponds that naturally disappear during the dry season in southeastern Africa. These environmental conditions have been proposed to influence life-cycle strategies within this species (Furness, 2016; Mazzetto et al., 2025; Terzibasi et al., 2008). In parallel, laboratory strains also differ in their genetic background. For example, the short-lived GRZ strain is a highly inbred strain maintained in captivity since the late 1960s and used in laboratory since the early 2000s, whereas MZCS-222 is a more recently established outbred strain with a longer lifespan (Reichwald et al., 2009; Valenzano et al., 2015). Together, these two strains provide a valuable model for investigating molecular mechanisms associated with differences in lifespan.

☆ This article is part of a Special issue entitled: 'Mitochondria, Aging, and the Brain' published in Experimental Gerontology.

* Corresponding author at: Croix du Sud, 5 Carnoy Building A2, 1348, Louvain-la-Neuve, Box: L7.07.03, Belgium.
*E-mail address:* melissa.page@uclouvain.be (M.M. Page).

[1] Authors contributed equally to the work.

https://doi.org/10.1016/j.exger.2026.113347
Received 5 June 2026; Received in revised form 24 September 2026; Accepted 5 October 2026
Available online 6 October 2026
0531-5565/© 2026 The Authors. Published by Elsevier Inc. This is an open access article under the CC BY license (http://creativecommons.org/licenses/by/4.0/).

Despite considerable progress in aging research, the molecular mechanisms underlying lifespan divergence remain incompletely understood. Among cellular processes implicated in aging, mitochondrial homeostasis appears particularly important as mitochondria are central regulators of cellular energy production, oxidative metabolism, and stress responses. In *N. furzeri*, mitochondrial function in skeletal muscle has already been reported to be impaired with age as assessed by a decrease in the protein content of complexes III and IV of the respiratory chain, as well as an overall reduction in mitochondrial respiration (Hartmann et al., 2011). More recently, proteomic and transcriptomic analysis of *N. furzeri* brains revealed a decoupling between transcripts and protein during aging. While ribosomal proteins were reduced and their transcripts were increased, OXPHOS gene expression was reduced but proteins were increased, revealing a remodeling of the mitochondrial proteome with age (Di Fraia et al., 2025).

Mitochondria are also the major producers of reactive oxygen species (ROS), which have been implicated in the accumulation of molecular damage during aging. For example, the oxidative stress theory of aging suggests that the progressive accumulation of oxidative damage contributes to the age-related decline of cellular function (Harman, 1956, 1972). Supporting this hypothesis, several studies have reported a negative correlation between ROS production and lifespan across several short- and long-lived species (Shields et al., 2021). Although, the oxidative stress theory has contributed to our understanding of aging mechanisms, it is now recognized as only a part of a more complex process, in which ROS also have essential signaling roles, promoting adaptative responses through mitohormesis (Baumgart et al., 2014; Costantini, 2024; López-Otín et al., 2023; Shields et al., 2021).

In this study, we took advantage of the contrasting lifespans of the short-lived GRZ strain, collected from Gonarezhou National Park in Zimbabwe (1969), and the longer-lived MZCS-222 strain, collected from Mozambique (2011) (Cellerino et al., 2016; Terzibasi et al., 2008). To better understand if distinct age-related patterns were associated with their divergent aging trajectories, we measured markers of oxidative damage, antioxidant defense protein levels and levels of key genes of mitophagy and apoptosis at young, adult, old and/or very old ages. We made our focus on the brain to strengthen current results that brain aging of *N. furzeri* acts as a model for human neurodegenerative diseases (de Bakker and Valenzano, 2023).

## 2. Methods

### 2.1. Animal care and tissue retrieval

All procedures were approved by the local Animal Ethics Committee of UCLouvain (Louvain-la-Neuve, Belgium; Agreement number LA1220587) in accordance with the European Communities Council Directive of 22 September 2010 (2010/63/EU) and the Belgian legislation (KB of 29 May 2013). GRZ and MZCS-222 *N. furzeri* were reared in 3.5 l ZebTEC Active Blue Standalone aquariums (Tecniplast, Italy) with a 12 h artificial day/night cycle, grouped either in a 1:3 male-to-female ratio or as two males separated by a perforated divider. System water was maintained at 28 °C, pH 7–7.5 and conductivity 650–710 μS. Fish were fed daily with thawed blood worm larvae (Chironomus spp.) and live *Artemia* nauplii. For lifespan analysis, a cohort of 81 GRZ fish (50 males, 31 females) and a cohort of 44 MZCS-222 fish (19 males, 25 females) were monitored daily. Death was recorded to generate Kaplan-Meier curves. In our facility, GRZ and MZCS-222 had a median lifespan of 19 and 30 weeks, respectively and a maximum lifespan (10% survival) of 28 and 41 weeks, respectively. Based on the Kaplan-Meier curves, we used the following comparative biological timepoints for GRZ and MZCS-222: young (6 weeks), adult (12 weeks), old (19 and 30 weeks) and very old (26 and 41 weeks) (Suppl. Fig. 1A–C). The oldest cohorts for GRZ were collected at 26 weeks in place of 28 weeks, to ensure enough biological replicates. *N. furzeri* were euthanized using 0.4% ethyl 3-aminobenzoate methanesulfonate (MS-222, Sigma-Aldrich). Brains were dissected, flash frozen in liquid nitrogen and stored at −80 °C until further use. Independent cohorts of fish were used for the different experiments because a single whole brain did not provide sufficient starting material for multiple downstream analyses (Suppl. Table 1). For RT-qPCR, RNA extracted from each whole brain was used to quantify all target genes.

### 2.2. Protein extraction

Whole brains were homogenized on ice in 200 μl RIPA buffer (50 mM Tris, 0.1% SDS, 150 mM NaCl, 0.25% sodium deoxycholate, 1% triton X-100, 1% protease inhibitor cocktail added fresh, pH 7.4) using a motor-driven grinder for 30 s, followed by 30 s incubation on ice. This was repeated three times. Homogenates were sonicated for 1 min and incubated on ice for 30 min. Samples were centrifuged (15 min, 15,300 g, 4 °C). Protein concentration was quantified for the collected supernatants following the Pierce™ BCA Protein Assay Kit (Thermo Fisher Scientific) protocol.

### 2.3. Western blot

Ten μg of protein was incubated for 5 min at 95 °C in loading buffer (125 mM Tris, 4% SDS, 20% glycerol, 0.004% bromophenol blue, 1% DTT, pH 6.8). Protein separation was performed within a 12% polyacrylamide gel using a PowerPac™ Basic power supply (Bio-Rad) set at 100 V for 20 min, then at 130 V for 90 min. Proteins were transferred (semi-dry, Invitrogen) from the gel to PVDF membranes at 20 V (45 min). Membranes were blocked with either 5% milk powder or 5% BSA in TBS-T (24 mM Tris, 192 mM NaCl, 0.1% TWEEN® 20, pH 7.6) for 45 min at room temperature (RT) followed by three washes in TBS-T and then incubated overnight with primary antibodies at 4 °C (Anti-Sod1: Abcam, ab13498, 1/1000; Anti-Sod2: Cell Signaling, 13194S, 1/1000; Anti-β-actin: Sigma-Aldrich, A2066, 1/100). The next day, membranes were washed three times in TBS-T, before a 1 h incubation with the secondary antibody (Goat anti-Rabbit: Invitrogen, 31466, 1/5000) at RT. Protein bands were detected using luminol (Sigma-Aldrich) or ClarityMax™ (Bio-Rad) in an Amersham™ Imager 600 (Cytiva, Belgium). Quantification of bands was performed using ImageJ software. β-Actin served as the loading control. To compare protein levels across several Western blots, a control sample was loaded onto each gel and used for normalization.

### 2.4. Citrate synthase activity

Citrate synthase (CS) activity was measured using a spectrophotometric assay at 412 nm. The reaction mix contained Triton X-100, acetyl-CoA and DTNB. For each sample, 20 ng protein were added, and a background absorbance was recorded for 2 min at RT. Oxaloacetate was added to initiate the reaction, and absorbance was measured every 15 s for 10 min. For each sample, the background absorbance was subtracted from all timepoints of the kinetics. The activity of CS was calculated using the slope of each curve that follows a linear regression.

### 2.5. RNA extraction and RT-qPCR

RNA extraction was performed using the Aurum™ Total RNA Mini Kit (Bio-Rad). Brains were homogenized in 0.5 ml TRIzol using a motor-driven grinder and then incubated at RT (5 min). Chloroform (0.1 ml) was added to the homogenized samples, and the tubes were shaken vigorously by hand for 15 s and centrifuged (15 min, 12,000 g, 4 °C). RNA was eluted from the columns by the addition of 40 μl elution solution. RNA quality and concentration were measured using a NanoDrop spectrophotometer (ND-1000; Thermo Fisher Scientific). RNA samples were stored at −80 °C until further use. The iScript™ cDNA synthesis kit (Bio-Rad) was used to synthesize cDNA, following the manufacturer's protocol. cDNA was stored at −20 °C until further use. GoTAQ qPCR

Master kit (Promega) was used to perform qPCR. Two µl cDNA were loaded in triplicates into a 96-well plate. Eighteen µl master mix (10 µl Promega GoTAQqPCR product, 0.2 µl Carboxy-X-Rhodamine, primers in the optimal concentration ratio (Suppl. Table 2) and nuclease-free water) were added to each cDNA sample. Two negative controls, "no RT" and "no cDNA", were included. cDNA was amplified using a StepOnePlus Instrument (Thermo Fisher Scientific) with standard cycling conditions. Mean $C_t$ values of each sample were determined, and the relative gene expression (RGE) was calculated for each condition (age) using the $\Delta\Delta C_t$ method.

### 2.6. DNA extraction and mitochondrial DNA copy number

DNA was extracted from *N. furzeri* brain tissue samples following manufacturer's instruction from the NucleoSpin® Tissue XS kit. After purification, DNA was eluted using 20 µl eluant buffer and stored at −20 °C until further use. DNA purity was first assessed using a NanoDrop spectrophotometer (ND-1000; Thermo Fisher Scientific). The absorbance ratios at 260/280 nm and 260/230 nm were measured to assess contamination and remove potential outliers.

Relative mitochondrial DNA (mtDNA) copy number was measured using the protocol proposed Hartmann et al. (2011). Real-time PCR was used and consists of the ratio of the mitochondrial 16S rRNA gene to the nuclear *Cdkn2a/b* gene locus. PCR amplification was performed with the StepOnePlus Instrument (Thermo Fisher Scientific) in 20 µl containing 10 µl Promega GoTAQqPCR product, 200 nM of each primer (Suppl. Table 3), nuclease free-water and 20 ng DNA. Thermal cycling conditions included a denaturation step at 95 °C (2 min) followed by 40 cycles of 95 °C for 15 s, 60 °C for 1 min and a melting curve from 60 to 95 °C with 0.3 °C step. All samples were loaded in triplicate as well as a negative control for each set of primers. $C_t$ values of mitochondrial 16 s rRNA were normalized to $C_t$ values of the nuclear locus Cdkn2a/b to obtain the relative mtDNA copy number per diploid cell using the following equation: Relative mtDNA copy number per diploid cell $= 2 * 2^{\Delta Ct}$, where $\Delta Ct = Ct_{,cdkn2a/b} - Ct_{,16s\ rRNA}$.

### 2.7. Lipid peroxidation

Lipid peroxidation was evaluated via malondialdehyde (MDA) concentration using a Lipid Peroxidation Assay Kit (MAK085, Sigma-Aldrich) with the following modifications. Whole brains were homogenized in 300 µl RIPA buffer and 3 µl BHT using a motor-driven grinder. Samples were centrifuged (10 min, 13,000 g, RT) and 200 µl supernatant was mixed with 600 µl TBA solution (7 mM TBA in glacial acetic acid and MilliQ water 3:10). Standards (0 to 10 nM MDA, in duplicates) were similarly processed. All tubes were incubated at 95 °C (60 min) then cooled on ice (10 min). Next, 300 µl 1-butanol and 100 µl 5 M NaCl were added to the samples and standards. After a quick vortex, samples were centrifuged (3 min, 16,000 g, RT). 200 µl of the upper phase was transferred to a 96-well black plate. Fluorescence at 532 nm/553 nm was measured with a Tecan Infinite 200 Pro fluorometer. Fluorescence of all standards and samples was corrected by subtracting the blank value. MDA molar amount in each sample was determined based on the standard curve using mean corrected fluorescence of duplicate standards. MDA concentration was calculated based on the manufacturer's protocol.

### 2.8. Protein carbonyl content

Protein carbonyl content was assessed via 2,4-dinitrophenylhydrazine derivatization using a Protein Carbonyl Content Assay Kit (MAK094, Sigma-Aldrich). Protein extracts were prepared from whole brains. 100 µl undiluted protein extracts were assayed following the manufacturer's instructions. Absorbance of obtained dinitrophenyl hydrazone adducts was measured at 375 nm using a Tecan Infinite 200 Pro spectrophotometer. Demineralized water was used as a blank. Protein carbonyl content was calculated based on the manufacturer's protocol.

### 2.9. SOD activity assay

Superoxide dismutase (SOD) activity was evaluated using a SOD Determination Kit (19,160, Sigma-Aldrich), with the following modifications. Brains were homogenized in 250 µl RIPA buffer (SDS free) using a motor-driven grinder for two times 30 s, resting 30 s on ice in between. The samples were centrifuged at 14,000 *g* (5 min, 4 °C). The supernatant was transferred to a new tube and serial dilutions were prepared (1/2, 1/4, 1/8, 1/16, 1/32). All undiluted samples, dilutions and blanks were assayed in a 96-well microplate following the kit's protocol. The microplate was mixed on a shaker (30 s), covered and incubated (20 min, 37 °C). After incubation, the plate was allowed to cool to RT before measuring absorbance at 450 nm on a SpectraMax190 Microplate Reader (United Kingdom). SOD activity was calculated based on the manufacturer's protocol.

### 2.10. Statistical analysis

Number of replicates for each age, sex and strain can be found in Suppl. Table 1. A two-way ANOVA did not reveal sex as a significant variable. Data were normalized to the young timepoint of each strain. GraphPad Prism software (11.0.0 version) was used for statistical analysis. Data were first tested for Gaussian normality and variance equality to ensure the appropriate choice of statistical tests. Student's *t*-tests for pairwise comparison and ordinary one-way ANOVAs with Sidak's multiple comparison tests were used to determine if there was a significant difference between the means of the different ages. Means were considered significantly different when $p \leq 0.05$.

## 3. Results

### 3.1. Levels of inner and outer mitochondrial membrane proteins decrease with age in short-lived GRZ fish

To assess whether mitochondrial content differed between the GRZ and MZCS-222 *N. furzeri* strains, we quantified protein levels of ATP5B and TOM20, which are associated with the inner and outer mitochondrial membrane respectively, and activity levels of CS. The activity of this enzyme has already been used in literature as a marker of mitochondrial content due to its exclusive mitochondrial localization (Larsen et al., 2012).

Both ATP5B and TOM20 protein levels were significantly decreased in the brain of old compared to young GRZ fish. In contrast, the levels of these two proteins did not differ between young and old MZCS-222 brains (Fig. 1A, B & C). To correct mitochondrial protein level by mitochondrial content, we calculated the geometric mean of ATP5B and TOM20 levels for each individual fish (Fig. 1D). To date, the activity of a mitochondrial enzyme has not been reported in *N. furzeri* in an aging context. Therefore, we assessed whether age affected the activity of CS in the same manner as it did for the protein levels of ATP5B and TOM20 protein. To our surprise, CS activity was significantly upregulated in the old brains compared to younger brains in both strains (Fig. 1E). Using ATP5B and TOM20B levels to normalize CS activity, the increase was more pronounced in old GRZ brains compared to MZCS-222 brains (Suppl. Fig. 2).

### 3.2. Age-related decline in mtDNA copy number is also specific to the short-lived GRZ strain

To further characterize age-related changes in mitochondrial abundance, we quantified mtDNA copy number in the brains of both strains. While the number of mtDNA copies remained relatively stable throughout aging in the brain of the long-lived MZCS-222 strain, a

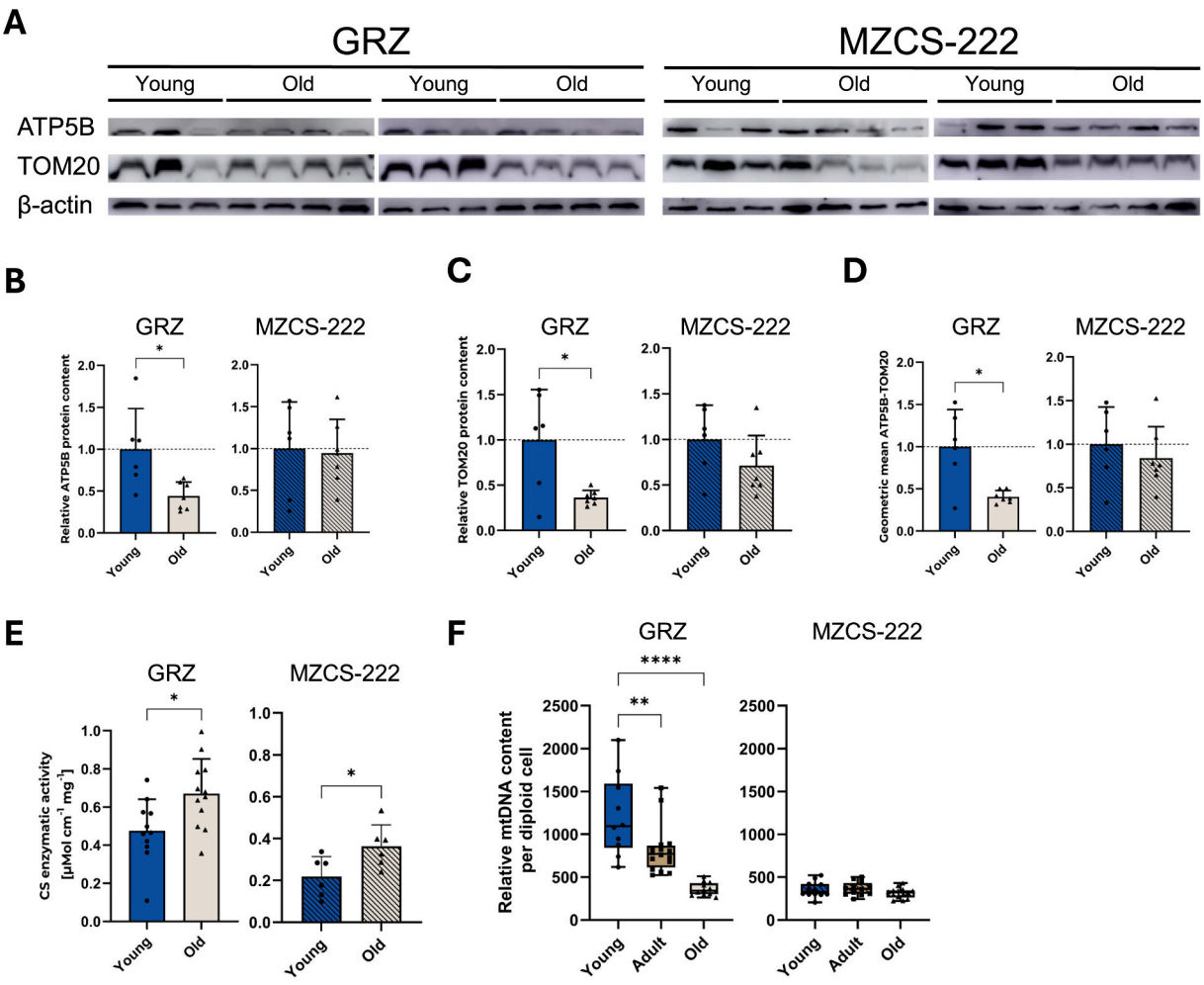



**Fig. 1.** Mitochondrial content is decreased with age in GRZ but not in MZCS-222. A) Western blot of ATP5B and TOM20 in GRZ and MZCS-222 brains at different ages. B) Protein levels of ATP5B in GRZ and MZCS-222 brains. C) Protein levels of TOM20 in GRZ and MZCS-222 brains. $N_{GRZ} = 6–8$, $N_{MZCS-222} = 6–8$. D) Geometric mean of ATP5B-TOM20 relative quantification. E) Citrate synthase activity. $N_{GRZ} = 6–8$, $N_{MZCS-222} = 6–8$. F) Mitochondrial DNA copy number in GRZ and MZCS-222 brains. $N_{GRZ} = 10–16$, $N_{MZCS-222} = 12–14$. Plain bars represent GRZ samples and hatched bars represent MZCS-222 samples. Bars represent the mean ± SD. Young = 6 weeks, Adult = 12 weeks, Old = 19/30 weeks for GRZ and MZCS-222 respectively. Asterisks indicate significant differences compared with the young group (* < 0.05, ** < 0.01, *** < 0.001, **** < 0.0001).

significant age-related decline was observed in the short-lived GRZ strain (Fig. 1F). It is interesting to note that young GRZ individuals had a higher number of mtDNA copies compared to young MZCS-222 strain (1205 vs 359 copies per diploid cell). This difference gradually disappeared with aging, as the number of mtDNA copies decreased in GRZ individuals until it reached 361 copies per cell in old fish which was similar to the 314 copies per cell measured in old MZCS-222 fish.

### 3.3. Markers of oxidative damage are increased with age in brains of short-lived GRZ fish

Along with a decrease in mitochondrial content, aging has been associated with increased oxidative damage (Jones and Brewer, 2010). To determine if reduced mitochondrial content in the brain of the short-lived GRZ strain is accompanied by increased oxidative damage, we measured markers of lipid and protein oxidation at two ages in the GRZ and MZCS-222 *N. furzeri* strains. Levels of MDA, which is a main product of polyunsaturated fatty acid peroxidation, were significantly higher in the brains of very old fish compared to those of young fish within the GRZ strain. In contrast, MDA levels were significantly lower in the brains of very old MZCS-222 fish compared to young individuals (Fig. 2A). Protein oxidation was assessed by measuring protein carbonyl levels, and like the MDA levels, these were also significantly elevated in older brains compared to young brains of the GRZ strain. In contrast, the level of protein carbonyls did not significantly differ between ages in the brain of the MZCS-222 strain (Fig. 2B).

### 3.4. Levels of SOD are increased with age in the brains of the long-lived MZCS-222 strain

Due to the differences in markers of oxidative damage between the two *N. furzeri* strains, we measured protein level and activity of SOD, the first line of defense that converts superoxide radicals into molecular oxygen and hydrogen peroxide (Ighodaro and Akinloye, 2018). While brain SOD1 and SOD2 protein levels did not differ between young and old GRZ fish, the levels were significantly elevated in old MZCS-222 fish (Fig. 2C, D & E). SOD1 is localised to the cytosol and mitochondrial intermembrane space, however SOD2 is found only within the mitochondrial matrix. Therefore, to account for mitochondrial content, SOD2 levels were normalized with the geometric mean of ATP5B and TOM20 levels. After normalization, SOD2 protein levels were significantly increased in the brains of old GRZ individuals and remained significantly elevated in the MZCS-222 (Fig. 2F). While these results indicate that the density of SOD2 per mitochondria was significantly

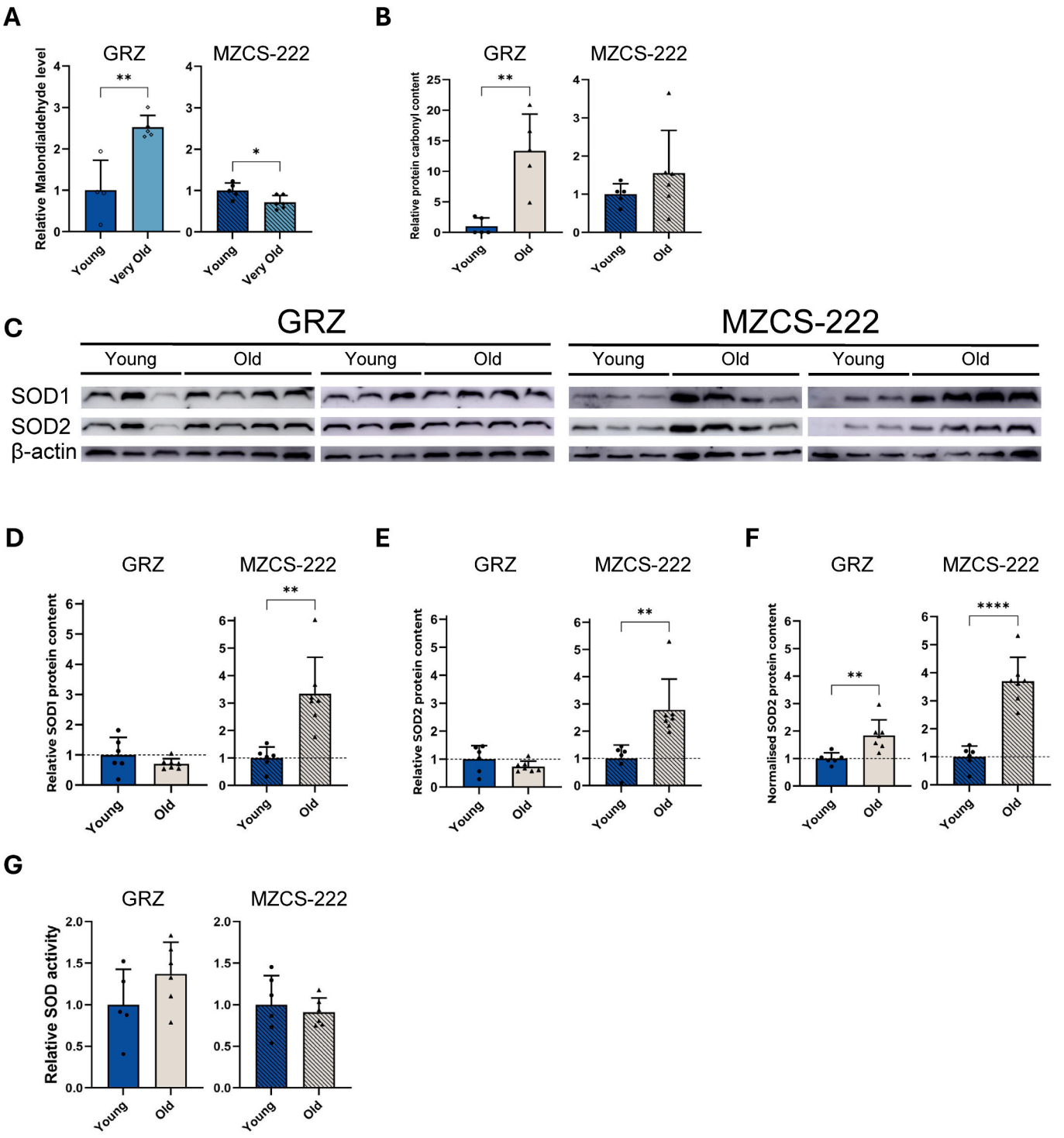



**Fig. 2.** Markers of oxidative stress are found in GRZ whereas SOD antioxidant increases in MZCS-222. A) MDA content measured by TBARS assay. $N_{GRZ} = 4–5$, $N_{MZCS-222} = 5–6$. B) Protein carbonyl content measured by DNPH derivatization. $N_{GRZ} = 4–5$, $N_{MZCS-222} = 5–6$. C, D & E) Protein levels of Sod1 and Sod2 measured by Western Blot and relative quantification. $N_{GRZ} = 6–7$, $N_{MZCS-222} = 6–7$. F) Normalization of SOD2 protein level by the geometric mean of ATP5B-TOM20. G) SOD activity levels measured by formazan inhibition. $N_{GRZ} = 5–6$, $N_{MZCS-222} = 6$. All data have been normalized with the young timepoint. Plain bars represent GRZ samples and hatched bars represent MZCS-222 samples. Bars represent the mean ± SD. Young = 6 weeks, Old = 19/30 weeks, Very Old = 26/41 weeks for GRZ and MZCS-222 respectively. Asterisks indicate significant differences compared with the young group (* < 0.05, ** < 0.01, *** < 0.001, **** < 0.0001).

increased in the old brains of both strains, protein level may not reflect the activity of the enzymes. Indeed, total SOD activity was stable with age in both strains (Fig. 2G).

### *3.5. Key mitophagy and apoptosis genes are recruited at younger age in the brains of GRZ*

To understand whether the increased oxidative damage and reduced SOD activity could be linked to the activation of mitophagy or apoptosis,

we analyzed mRNA levels of *pink1* (mitophagy signaling protein), *bcl2* (anti-apoptotic protein) and *bax* (pro-apoptotic protein) in both strains using RT-qPCR. Expression levels of *pink1* were significantly upregulated in the adult of the GRZ strain compared to the young brain. A similar upregulation was observed in the MZCS-222 strain, but only between the adult and very old age groups (Fig. 3A). Expression levels of *bax* were significantly increased from young to adult and very older brains of the GRZ strain, whereas no significant changes were observed in the brains of the MZCS-222 strain (Fig. 3B). The expression levels of *bcl2* were stable across all age groups in both strains (Fig. 3C).

## 4. Discussion

The lifespan divergence between these two strains remains in a lab setting years after collection, suggesting that cellular and/or molecular mechanisms are also partly responsible for strain longevity. To explore whether this was due to mitochondrial adaptations, we measured mitochondrial content, markers of oxidative damage and markers associated with oxidative damage response.

To assess changes in mitochondrial content, we measured the protein levels of ATP5B and TOM20 as well as quantified mtDNA copy number. ATP5B is a catalytic subunit of ATP synthase located in the inner mitochondrial membrane and is central to oxidative phosphorylation and ATP production. TOM20 is a translocase located in the outer mitochondrial membrane involved in mitochondrial import of nuclear-encoded proteins. ATP5B and TOM20 have previously been used to estimate mitochondrial content (Cacciottola et al., 2026; Esparza-Moltó et al., 2025; Sharapova et al., 2024). In addition, mtDNA copy number is widely used as a proxy for mitochondrial abundance (Larsen et al., 2012; Short et al., 2005). Together, the results from these complementary approaches indicate that GRZ fish exhibit a significant decrease in brain mitochondrial content with age, which is not the case for MZCS-222 fish.

The preservation of mitochondrial content in the longer-lived MZCS-222 strain may reflect a greater capacity to maintain mitochondrial homeostasis and energy metabolism during aging, which could contribute to its slower aging trajectory and longer lifespan although our study does not establish a causal relationship (Guo et al., 2023; Lanza and Nair, 2010). In contrast, the progressive decline observed in GRZ aligns with the age-related loss of mitochondria reported during aging in several vertebrate species, due to the accumulation of ROS-induced damage (Bratic and Larsson, 2013; Conley et al., 2000; Short et al., 2005). A previous study reported an age-related decline in brain mtDNA copy number in another longer-lived *N. furzeri* strain (MZM-0403) (Hartmann et al., 2011). However, in the present study copy number remained stable in the longer-lived MZCS-222, suggesting that mitochondrial homeostasis during aging may vary among *N. furzeri* strains.

One notable finding was the significantly higher mtDNA copy number observed in young GRZ fish compared to young MZCS-222 individuals. This may indicate distinct early-life mitochondrial profiles between strains with different aging trajectories. Previous studies have demonstrated that short- and longer-lived *N. furzeri* strains exhibit different age-dependent transcriptional profiles, with molecular differences already observable in the early stages of life (Mazzetto et al., 2025; Petzold et al., 2013). Furthermore, differences in gene expression early in life in *N. furzeri* have been associated with longevity, with genes related to mitochondrial complex I appearing closely linked to lifespan (Baumgart et al., 2016). Similarly, genes involved in mitochondrial biogenesis and function have undergone positive selection in short-lived *Nothobranchius* lineages (Sahm et al., 2017). Together, these observations suggest that mitochondrial regulation may contribute to the distinct aging trajectories observed between strains. While our data does not directly demonstrate a trade-off between early- and late-life fitness, recent work in *N. furzeri* identified *vestigial-like 3* (*vgll3*) as an antagonistic pleiotropic gene having opposing effects across life stages (Moses et al., 2026).

In both strains, and contrary to ATP5B and TOM20 protein levels and mtDNA copy number, CS activity increased with age. CS activity has historically been used to assess mitochondrial content (Larsen et al., 2012; Page et al., 2009; Vigelsø et al., 2014). However, recent evidence has questioned its reliability as a marker for mitochondrial content and that changes in its activity may not reflect changes in mitochondrial mass (Marin-Garcia et al., 1998; McLaughlin et al., 2020). This may be the case for *N. furzeri* brains, and that the increase in CS activity with age may reflect a compensatory response to mitochondrial function rather than mitochondrial content. Considering this, we corrected CS activity by ATP5B and TOM20 protein levels. We believe that the dramatic four-fold increase of normalized CS activity in GRZ may occur to compensate for the loss of mitochondria. However, this increased enzyme activity may promote an increase in ROS production and higher levels of damaged mitochondria. In contrast, the slight two-fold increase of normalized CS activity in the brains of the MZSC-222 fish along with the stability of mitochondrial markers may reflect an improved regulation of mitochondrial homeostasis.

A decrease in mitochondrial content may be linked to an increased level of oxidative damage (Bratic and Larsson, 2013; Jones and Brewer, 2010). Indeed, we observed an increase in both MDA and protein carbonyl levels in the brains of old GRZ individuals. In contrast, MDA levels were decreased and protein carbonyl content remained stable in old MZCS-222 brains. MDA levels have also been reported to decrease with age in the liver of old MZM-0410 individuals. However, this was not the case in skeletal muscle where levels increased between young and old fish (Milinkovitch et al., 2018). These results may suggest that

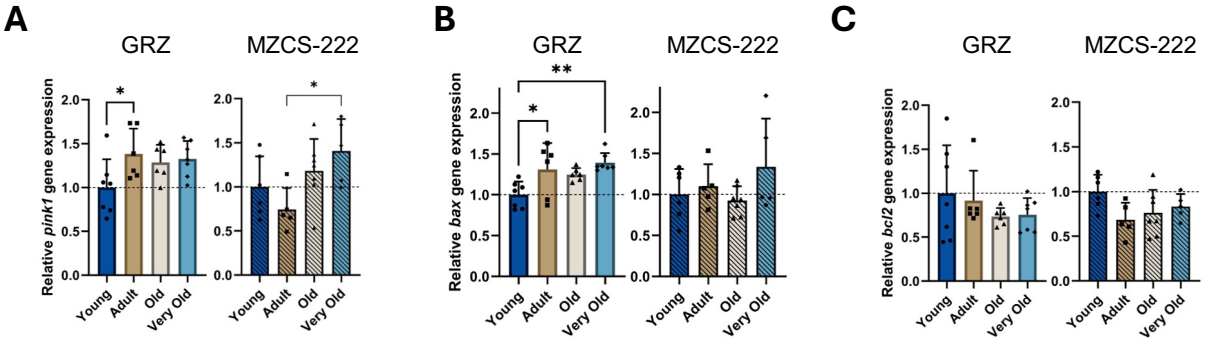



**Fig. 3.** Key mitophagy and apoptosis genes are recruited at younger ages in the brains of GRZ. Relative gene expression measured by RT-qPCR of A) *pink1*, mitophagy signaling protein B) *bax*, pro-apoptotic protein C) *bcl2*, anti-apoptotic protein. $N_{GRZ}$ = 6–8, $N_{MZCS\text{-}222}$ = 6–8. Plain bars represent GRZ samples and hatched bars represent MZCS-222 samples. Young = 6 weeks, Adult = 12 weeks Old = 19/30 weeks, Very Old = 26/41 weeks for GRZ and MZCS-222 respectively. Bars represent the mean ± SD. Asterisks indicate significant differences compared with the young group (* < 0.05, ** < 0.01).

lipid peroxidation is organ-specific and/or strain-specific. Lower lipid peroxidation and stable protein carbonylation corroborates the hypothesis that the longer lifespan of MZCS-222 fish is associated with a better management of oxidative damage. Lower MDA and protein carbonyl levels have previously been reported in long-lived vertebrate models compared to short-lived species (Bhattacharya et al., 2011; Jové et al., 2020).

Due to the age-related increase in markers of oxidative damage in old GRZ brains, we asked ourselves if this could be due to impaired antioxidant capacity of SOD, which is considered the first line of defense against ROS. While SOD1 protein levels remained unchanged between the different ages in the GRZ strain, SOD2 protein levels significantly increased when corrected for mitochondrial content (based on protein levels of ATP5B and TOM20).

Several lines of evidence have revealed a positive correlation between antioxidant enzymes and lifespan (Liu et al., 2012; Page et al., 2010). In contrast to the GRZ strain, SOD1 and SOD2 proteins levels are upregulated with age in the MZCS-222 strain, in the latter case before and after correction for mitochondrial content. This may represent a mechanism to counteract oxidative damage associated with its longer lifespan, which may explain the stable levels of oxidative damage markers observed in this strain (Barja, 2002). Total SOD activity remained stable with age in both strains; nevertheless, MZCS-222 may maintain a higher overall superoxide detoxification capacity across aging due to increased levels of SOD1 and SOD2 compared to GRZ.

When oxidative stress can no longer be efficiently counteracted by antioxidant defenses and mitochondrial maintenance systems, damaged cells may activate others protection pathways such as mitophagy or in severe cases, apoptosis. In general, aging is associated with a progressive decline in antioxidant capacity and mitochondrial quality control, contributing to the accumulation of dysfunctional mitochondria and increased susceptibility to apoptosis (Kang et al., 2020). In this context, PINK1, BAX and BCL-2 are key proteins of complementary mitochondrial stress responses. PINK1 accumulates in the outer mitochondrial membrane of damaged mitochondria, where it autophosphorylates and acts as a kinase to phosphorylate Parkin, triggering mitophagy (Lambourne et al., 2023). During aging, insufficient mitochondrial turnover via mitophagy can lead to adaptive responses toward pro-apoptotic signaling (Gautier et al., 2008; Green and Reed, 1998). The balance between BAX (pro-apoptotic) and BCL-2 (anti-apoptotic) plays a key role in the regulation of mitochondrial apoptosis (Putri and Z, 2025). In aging, this imbalance indicates a greater sensibility to apoptosis due to endogenous stress, leading to mitochondrial function decline (Elias, 2018; Xu et al., 2025).

In GRZ, we observed an upregulation of *pink1* and *bax* gene expression at the adult stage. This may indicate an insufficient removal of damaged mitochondria through mitophagy and a greater need to eliminate cells with damaged mitochondria through apoptosis. In the liver of *N. furzeri* (GRZ), the proportion of cells exhibiting apoptosis increased more rapidly with age compared to *N. kadleci*, a longer-lived *Nothobranchius* species (Ng'oma et al., 2014). In a proteomic analysis of GRZ plasma, apoptosis was a GO term highly enriched in old vs young individuals (Morabito et al., 2026). Finally, proteomic analysis of telencephalon has also shown that proteins of apoptosis KEGG pathway were increased in the GRZ aged group compared to the young group (Van houcke et al., 2023). Taken together, those data reinforce our hypothesis that apoptosis is increased with age in GRZ. Such activation of apoptotic pathways may be associated with the age-related decline in mitochondrial content observed in this strain in order to eliminate dysfunctional mitochondria. In contrast, in the MZCS-222 strain, oxidative stress may be better managed, as we observed a gradual age-related upregulation of *pink1*, suggesting an activation of mitophagy to eliminate damaged mitochondria. At the same time, *bax* expression levels remained stable, which may indicate that apoptosis is not strongly triggered in the MZCS-222 strain, even at very old ages. Exploring the proteomics data of MZM-0410 brains, BAX was decreased in older individuals of this other longer-lived strain (Di Fraia et al., 2025). Together with our results that indicate stable mitochondrial content, it appears that mitochondrial homeostasis is maintained through selective removal of damaged mitochondria rather than apoptosis, though this would need to be verified.

## 5. Conclusion

Taken together, our results suggest that the longer lifespan of MZCS-222 killifish may be associated with a greater capacity to maintain mitochondrial homeostasis through aging. Compared to the short-lived GRZ strain, MZCS-222 had higher levels of antioxidant defenses, as indicated by the upregulation of SOD1 and SOD2 levels, which may have contributed to the mitigation of the oxidative damage markers. In parallel, the age-related increase in *pink1* expression and maintenance of *bax* suggest enhanced mitochondrial quality control via mitophagy without special need for apoptosis. In contrast, individuals from the GRZ strain appeared more vulnerable to oxidative stress, with significantly increased levels of MDA and protein carbonyl during aging. They also exhibited a decrease in mitochondrial abundance and a significant increase in *bax* levels early in life. These alterations could be explained by the progressive inability of antioxidants defenses to control ROS levels during aging. When ROS levels exceed the threshold to promote mitohormesis, oxidative damage accumulates and can trigger a vicious cycle of mitochondrial dysfunction and loss of mitochondrial content.

Our findings are consistent with the current view on aging, which propose mitochondrial dysfunction and the progressive decline of cellular maintenance as important contributors of the aging process (Fuentealba et al., 2021; López-Otín et al., 2023). Our study also aligned with evidence across diverse animal models detailing how long-lived species tend to have greater resilience to cellular stress and more efficient maintenance and antioxidant mechanisms compared to short-lived species (Barja, 2002; Pamplona and Barja, 2011).

Our results provide correlative evidence between mitochondrial homeostasis and lifespan difference in the two *N. furzeri* strains. To strengthen our molecular findings, additional functional mitochondrial measurements (i.e. oxygen consumption, mitochondrial ROS production) would provide complementary information but due to the relative newness of *N. furzeri* as a model organism, there are technical challenges that remain to be overcome.

## CRediT authorship contribution statement

**Julien Lehmann:** Writing – review & editing, Writing – original draft, Visualization, Validation, Methodology, Investigation, Formal analysis, Data curation, Conceptualization. **Oksana Savel:** Writing – review & editing, Writing – original draft, Visualization, Validation, Methodology, Investigation, Formal analysis, Data curation, Conceptualization. **Melissa M. Page:** Writing – review & editing, Supervision, Funding acquisition, Conceptualization.

## Funding

The authors gratefully acknowledge the support of the Fonds de la Recherche Scientifique (FRS-FNRS) through a FRIA doctoral fellowship for Julien Lehmann.

## Declaration of competing interest

The authors declare that they have no known competing financial interests or personal relationships that could have appeared to influence the work reported in this paper.

## Acknowledgements

We thank the killifish research team and specifically Cécile Gardin

and Ineke Neefs for the maintenance of the fish facility. The authors thank the ANCA platform (UCLouvain, LLN) for its support and for providing access to animal care and housing facilities.

## Appendix A. Supplementary data

Supplementary data to this article can be found online at https://doi.org/10.1016/j.exger.2026.113347.

## Data availability

No data was used for the research described in the article.

## References


Barja, G., 2002. Rate of generation of oxidative stress-related damage and animal longevity. Free Radic. Biol. Med. 33 (9), 1167–1172. https://doi.org/10.1016/S0891-5849(02)00910-3.

Baumgart, M., Groth, M., Priebe, S., Savino, A., Testa, G., Dix, A., Ripa, R., Spallotta, F., Gaetano, C., Ori, M., Terzibasi Tozzini, E., Guthke, R., Platzer, M., Cellerino, A., 2014. RNA-seq of the aging brain in the short-lived fish N. furzeri – conserved pathways and novel genes associated with neurogenesis. Aging Cell 13 (6), 965–974. https://doi.org/10.1111/acel.12257.

Baumgart, M., Priebe, S., Groth, M., Hartmann, N., Menzel, U., Pandolfini, L., Koch, P., Felder, M., Ristow, M., Englert, C., Guthke, R., Platzer, M., Cellerino, A., 2016. Longitudinal RNA-Seq analysis of vertebrate aging identifies mitochondrial complex I as a small-molecule-sensitive modifier of lifespan. Cell Syst. 2 (2), 122–132. https://doi.org/10.1016/j.cels.2016.01.014.

Bhattacharya, A., Leonard, S., Tardif, S., Buffenstein, R., Fischer, K.E., Richardson, A., Austad, S.N., Chaudhuri, A.R., 2011. Attenuation of liver insoluble protein carbonyls: indicator of a longevity determinant? Aging Cell 10 (4), 720–723. https://doi.org/10.1111/j.1474-9726.2011.00712.x.

Bratic, A., Larsson, N.-G., 2013. The role of mitochondria in aging. J. Clin. Invest. 123 (3), 951–957. https://doi.org/10.1172/JCI64125.

Cacciottola, L., Zhang, M., Houeis, L., Bouzin, C., van Dievoet, M.-A., Luyckx, M., Donnez, J., Dolmans, M.-M., 2026. Age-related changes in mitochondrial markers and telomere dynamics during initial growth of human preantral follicles. J. Assist. Reprod. Genet. 43 (1), 293–306. https://doi.org/10.1007/s10815-025-03721-0.

Cellerino, A., Valenzano, D.R., Reichard, M., 2016. From the bush to the bench: the annual Nothobranchius fishes as a new model system in biology. Biol. Rev. 91 (2), 511–533. https://doi.org/10.1111/brv.12183.

Conley, K.E., Jubrias, S.A., Esselman, P.C., 2000. Oxidative capacity and ageing in human muscle. J. Physiol. 526 (Pt 1), 203–210. https://doi.org/10.1111/j.1469-7793.2000.t01-1-00203.x.

Costantini, D., 2024. The long and the short of it: how oxidative stress drives cellular senescence, ageing, and lifespan of animals. In: Costantini, D. (Ed.), The Role of Organismal Oxidative Stress in the Ecology and Life-history Evolution of Animals. Springer Nature Switzerland, pp. 369–418. https://doi.org/10.1007/978-3-031-65183-0_10.

de Bakker, D.E.M., Valenzano, D.R., 2023. Turquoise killifish: a natural model of age-dependent brain degeneration. Ageing Res. Rev. 90, 102019. https://doi.org/10.1016/j.arr.2023.102019.

Di Fraia, D., Marino, A., Lee, J.H., Kelmer Sacramento, E., Baumgart, M., Bagnoli, S., Balla, T., Schalk, F., Kamrad, S., Guan, R., Caterino, C., Giannuzzi, C., Tomaz da Silva, P., Sahu, A.K., Gut, H., Siano, G., Tiessen, M., Terzibasi-Tozzini, E., Fornasiero, E.F., Gagneur, J., Englert, C., Patil, K.R., Correia-Melo, C., Nedialkova, D. D., Frydman, J., Cellerino, A., Ori, A., 2025. Altered translation elongation contributes to key hallmarks of aging in the killifish brain. Science 389 (6759), eadk3079. https://doi.org/10.1126/science.adk3079.

Elias, W.Y., 2018. Age-dependent differential expression of apoptotic markers in rat oral mucosa. Asian Pac. J. Cancer Prev. 19 (11), 3245–3250. https://doi.org/10.31557/APJCP.2018.19.11.3245.

Esparza-Moltó, P.B., Goswami, A.V., Bozkurt, S., Münch, C., Newman, L.E., Moyzis, A.G., Rojas, G.R., Guan, D., Jones, J.R., Gage, F.H., Shadel, G.S., 2025. ROS-dependent localization of glycolytic enzymes to mitochondria. Redox Biol. 86, 103812. https://doi.org/10.1016/j.redox.2025.103812.

Fuentealba, M., Fabian, D.K., Dönertaş, H.M., Thornton, J.M., Partridge, L., 2021. Transcriptomic profiling of long- and short-lived mutant mice implicates mitochondrial metabolism in ageing and shows signatures of normal ageing in progeroid mice. Mech. Ageing Dev. 194, 111437. https://doi.org/10.1016/j.mad.2021.111437.

Furness, A.I., 2016. The evolution of an annual life cycle in killifish: adaptation to ephemeral aquatic environments through embryonic diapause. Biol. Rev. 91 (3), 796–812. https://doi.org/10.1111/brv.12194.

Gautier, C.A., Kitada, T., Shen, J., 2008. Loss of PINK1 causes mitochondrial functional defects and increased sensitivity to oxidative stress. Proc. Natl. Acad. Sci. 105 (32), 11364–11369. https://doi.org/10.1073/pnas.0802076105.

Green, D.R., Reed, J.C., 1998. Mitochondria and apoptosis. Science 281 (5381), 1309–1312. https://doi.org/10.1126/science.281.5381.1309.

Guo, Y., Guan, T., Shafiq, K., Yu, Q., Jiao, X., Na, D., Li, M., Zhang, G., Kong, J., 2023. Mitochondrial dysfunction in aging. Ageing Res. Rev. 88, 101955. https://doi.org/10.1016/j.arr.2023.101955.

Harman, D., 1956. Aging: a theory based on free radical and radiation chemistry. J. Gerontol. 11 (3), 298–300. https://doi.org/10.1093/geronj/11.3.298.

Harman, D., 1972. The biologic clock: the mitochondria? J. Am. Geriatr. Soc. 20 (4), 145–147. https://doi.org/10.1111/j.1532-5415.1972.tb00787.x.

Hartmann, N., Reichwald, K., Wittig, I., Dröse, S., Schmeisser, S., Lück, C., Hahn, C., Graf, M., Gausmann, U., Terzibasi, E., Cellerino, A., Ristow, M., Brandt, U., Platzer, M., Englert, C., 2011. Mitochondrial DNA copy number and function decrease with age in the short-lived fish Nothobranchius furzeri. Aging Cell 10 (5), 824–831. https://doi.org/10.1111/j.1474-9726.2011.00723.x.

Hu, C.-K., Brunet, A., 2018. The African turquoise killifish: a research organism to study vertebrate aging and diapause. Aging Cell 17 (3), e12757. https://doi.org/10.1111/acel.12757.

Ighodaro, O.M., Akinloye, O.A., 2018. First line defence antioxidants-superoxide dismutase (SOD), catalase (CAT) and glutathione peroxidase (GPX): their fundamental role in the entire antioxidant defence grid. Alex. J. Med. 54 (4), 287–293. https://doi.org/10.1016/j.ajme.2017.09.001.

Jones, T.T., Brewer, G.J., 2010. Age-related deficiencies in complex I endogenous substrate availability and reserve capacity of complex IV in cortical neuron electron transport. Biochim. Biophys. Acta 1797 (2), 167–176. https://doi.org/10.1016/j.bbabio.2009.09.009.

Jové, M., Mota-Martorell, N., Pradas, I., Martín-Gari, M., Ayala, V., Pamplona, R., 2020. The advanced lipoxidation end-product malondialdehyde-lysine in aging and longevity. Antioxidants 9 (11), 1132. https://doi.org/10.3390/antiox9111132.

Kang, L., Liu, S., Li, J., Tian, Y., Xue, Y., Liu, X., 2020. Parkin and Nrf2 prevent oxidative stress-induced apoptosis in intervertebral endplate chondrocytes via inducing mitophagy and anti-oxidant defenses. Life Sci. 243, 117244. https://doi.org/10.1016/j.lfs.2019.117244.

Kirkwood, T.B.L., Austad, S.N., 2000. Why do we age? Nature 408 (6809), 233–238. https://doi.org/10.1038/35041682.

Lambourne, O.A., Bell, S., Wilhelm, L.P., Yarbrough, E.B., Holly, G.G., Russell, O.M., Alghamdi, A.M., Fdel, A.M., Varricchio, C., Lane, E.L., Ganley, I.G., Jones, A.T., Goldberg, M.S., Mehellou, Y., 2023. PINK1-dependent mitophagy inhibits elevated ubiquitin phosphorylation caused by mitochondrial damage. J. Med. Chem. 66 (11), 7645–7656. https://doi.org/10.1021/acs.jmedchem.3c00555.

Lanza, I.R., Nair, K.S., 2010. Mitochondrial function as a determinant of life span. Pflugers Arch. Eur. J. Physiol. 459 (2), 277–289. https://doi.org/10.1007/s00424-009-0724-5.

Larsen, S., Nielsen, J., Hansen, C.N., Nielsen, L.B., Wibrand, F., Stride, N., Schroder, H.D., Boushel, R., Helge, J.W., Dela, F., Hey-Mogensen, M., 2012. Biomarkers of mitochondrial content in skeletal muscle of healthy young human subjects. J. Physiol. 590 (14), 3349–3360. https://doi.org/10.1113/jphysiol.2012.230185.

Liu, C., Wang, X., Feng, W., Li, G., Su, F., Zhang, S., 2012. Differential expression of aging biomarkers at different life stages of the annual fish Nothobranchius guentheri. Biogerontology 13 (5), 501–510. https://doi.org/10.1007/s10522-012-9395-2.

López-Otín, C., Blasco, M.A., Partridge, L., Serrano, M., Kroemer, G., 2023. Hallmarks of aging: an expanding universe. Cell 186 (2), 243–278. https://doi.org/10.1016/j.cell.2022.11.001.

Marin-Garcia, J., Ananthakrishnan, R., Goldenthal, M.J., 1998. Human mitochondrial function during cardiac growth and development. Mol. Cell. Biochem. 179 (1–2), 21–26. https://doi.org/10.1023/a:1006839831141.

Mazzetto, M., Reichwald, K., Koch, P., Groth, M., Cellerino, A., 2025. Analysis of different strains of the turquoise killifish identify transcriptomic signatures associated with heritable lifespan differences. J. Gerontol. Ser. A 80 (7), glae255. https://doi.org/10.1093/gerona/glae255.

McLaughlin, K.L., Hagen, J.T., Coalson, H.S., Nelson, M.A.M., Kew, K.A., Wooten, A.R., Fisher-Wellman, K.H., 2020. Novel approach to quantify mitochondrial content and intrinsic bioenergetic efficiency across organs. Sci. Rep. 10, 17599. https://doi.org/10.1038/s41598-020-74718-1.

Milinkovitch, T., Lefrançois, C., Durollet, M., Thomas-Guyon, H., 2018. Influence of temperature on age-related lipid peroxidation in a short-lived vertebrate (Nothobranchius furzeri). Fish Physiol. Biochem. 44 (1), 343–347. https://doi.org/10.1007/s10695-017-0439-z.

Monaghan, P., Charmantier, A., Nussey, D.H., Ricklefs, R.E., 2008. The evolutionary ecology of senescence. Funct. Ecol. 22 (3), 371–378. https://doi.org/10.1111/j.1365-2435.2008.01418.x.

Morabito, G., Dönertas, H.M., Sperti, L., Seidel, J., Poursadegh Zonouzi, A., Poeschla, M., Valenzano, D.R., 2026. Spontaneous aging-associated inflammation and genome instability in the immune system of turquoise killifish. Nat. Aging 6 (3), 665–681. https://doi.org/10.1038/s43587-026-01086-2.

Moses, E., Bergman, M., Atlan, T., Duxbury, E.M.L., Franěk, R., Ben Dor, O., von Chrzanowski, H., Abu-Zhayia, E.R., Ayoub, N., Kinreich, S., Ben-Ami, I., Maklakov, A.A., Harel, I., 2026. An antagonistically pleiotropic gene regulates vertebrate growth, maturity, and lifespan. Nat. Commun. 17 (1), 4410. https://doi.org/10.1038/s41467-026-72381-0.

Ng'oma, E., Reichwald, K., Dorn, A., Wittig, M., Balschun, T., Franke, A., Platzer, M., Cellerino, A., 2014. The age related markers lipofuscin and apoptosis show different genetic architecture by QTL mapping in short-lived Nothobranchius fish. Aging 6 (6), 468–480. https://doi.org/10.18632/aging.100660.

Page, M.M., Peters, C.W., Staples, J.F., Stuart, J.A., 2009. Intracellular antioxidant enzymes are not globally upregulated during hibernation in the major oxidative tissues of the 13-lined ground squirrel Spermophilus tridecemlineatus. Comp. Biochem. Physiol. A Mol. Integr. Physiol. 152 (1), 115–122. https://doi.org/10.1016/j.cbpa.2008.09.032.

Page, M.M., Richardson, J., Wiens, B.E., Tiedtke, E., Peters, C.W., Faure, P.A., Burness, G., Stuart, J.A., 2010. Antioxidant enzyme activities are not broadly

correlated with longevity in 14 vertebrate endotherm species. AGE 32 (2), 255–270. https://doi.org/10.1007/s11357-010-9131-2.

Pamplona, R., Barja, G., 2011. An evolutionary comparative scan for longevity-related oxidative stress resistance mechanisms in homeotherms. Biogerontology 12 (5), 409–435. https://doi.org/10.1007/s10522-011-9348-1.

Petzold, A., Reichwald, K., Groth, M., Taudien, S., Hartmann, N., Priebe, S., Shagin, D., Englert, C., Platzer, M., 2013. The transcript catalogue of the short-lived fish Nothobranchius furzeriprovides insights into age-dependent changes of mRNA levels. BMC Genomics 14 (1), 185. https://doi.org/10.1186/1471-2164-14-185.

Polačik, M., Blažek, R., Řežucha, R., Vrtílek, M., Terzibasi Tozzini, E., Reichard, M., 2014. Alternative intrapopulation life-history strategies and their trade-offs in an African annual fish. J. Evol. Biol. 27 (5), 854–865. https://doi.org/10.1111/jeb.12359.

Putri, G.F.T., Z, Z.N., 2025. Bax/Bcl-2 ratio as the golden marker of apoptosis: molecular mechanisms and regulatory pathways. Int. J. Cell Biomed. Sci. 4 (10), 309–317. https://doi.org/10.59278/cbs.v4i10.65.

Reichwald, K., Lauber, C., Nanda, I., Kirschner, J., Hartmann, N., Schories, S., Gausmann, U., Taudien, S., Schilhabel, M.B., Szafranski, K., Glöckner, G., Schmid, M., Cellerino, A., Schartl, M., Englert, C., Platzer, M., 2009. High tandem repeat content in the genome of the short-lived annual fish Nothobranchius furzeri: a new vertebrate model for aging research. Genome Biol. 10 (2), R16. https://doi.org/10.1186/gb-2009-10-2-r16.

Reznick, D.A., Bryga, H., Endler, J.A., 1990. Experimentally induced life-history evolution in a natural population. Nature 346 (6282), 357–359. https://doi.org/10.1038/346357a0.

Sahm, A., Bens, M., Platzer, M., Cellerino, A., 2017. Parallel evolution of genes controlling mitonuclear balance in short-lived annual fishes. Aging Cell 16 (3), 488–496. https://doi.org/10.1111/acel.12577.

Savel, O., Lehmann, J., Poyraz, Y.K., Page, M.M., 2026. A short-lived fish with long-lasting effects: hallmarks of aging in Nothobranchius furzeri. Front. Aging 6. https://doi.org/10.3389/fragi.2025.1741819.

Sharapova, G., Sabirova, S., Gomzikova, M., Brichkina, A., Barlev, N.A., Kalacheva, N.V., Rizvanov, A., Markov, N., Simon, H.-U., 2024. Mitochondrial protein density, biomass, and bioenergetics as predictors for the efficacy of glioma treatments. Int. J. Mol. Sci. 25 (13), 7038. https://doi.org/10.3390/ijms25137038.

Shields, H.J., Traa, A., Van Raamsdonk, J.M., 2021. Beneficial and detrimental effects of reactive oxygen species on lifespan: a comprehensive review of comparative and experimental studies. Front. Cell Dev. Biol. 9. https://doi.org/10.3389/fcell.2021.628157.

Short, K.R., Bigelow, M.L., Kahl, J., Singh, R., Coenen-Schimke, J., Raghavakaimal, S., Nair, K.S., 2005. Decline in skeletal muscle mitochondrial function with aging in humans. Proc. Natl. Acad. Sci. 102 (15), 5618–5623. https://doi.org/10.1073/pnas.0501559102.

Terzibasi, E., Valenzano, D.R., Benedetti, M., Roncaglia, P., Cattaneo, A., Domenici, L., Cellerino, A., 2008. Large differences in aging phenotype between strains of the short-lived annual fish Nothobranchius furzeri. PLoS One 3 (12), e3866. https://doi.org/10.1371/journal.pone.0003866.

Valenzano, D.R., Benayoun, B.A., Singh, P.P., Zhang, E., Etter, P.D., Hu, C.-K., Clément-Ziza, M., Willemsen, D., Cui, R., Harel, I., Machado, B.E., Yee, M.-C., Sharp, S.C., Bustamante, C.D., Beyer, A., Johnson, E.A., Brunet, A., 2015. The African turquoise killifish genome provides insights into evolution and genetic architecture of lifespan. Cell 163 (6), 1539–1554. https://doi.org/10.1016/j.cell.2015.11.008.

Van Houcke, J., Mariën, V., Zandecki, C., Ayana, R., Pepermans, E., Boonen, K., Seuntjens, E., Baggerman, G., Arckens, L., 2023. A short dasatinib and quercetin treatment is sufficient to reinstate potent adult neuroregenesis in the aged killifish. npj Regener. Med. 8, 31. https://doi.org/10.1038/s41536-023-00304-4.

Vigelsø, A., Andersen, N.B., Dela, F., 2014. The relationship between skeletal muscle mitochondrial citrate synthase activity and whole body oxygen uptake adaptations in response to exercise training. Int. J. Physiol. Pathophysiol. Pharmacol. 6 (2), 84–101.

Williams, G.C., 1957. Pleiotropy, natural selection, and the evolution of senescence. Sci. Aging Knowl. Environ. 2001 (1), 398–411. https://doi.org/10.1126/sageke.2001.1.cp13.

Xu, X., Pang, Y., Fan, X., 2025. Mitochondria in oxidative stress, inflammation and aging: from mechanisms to therapeutic advances. Signal Transduct. Target. Ther. 10 (1), 190. https://doi.org/10.1038/s41392-025-02253-4.